BLOCK COPOLYMERS AS COMPATIBILIZERS IN COARSENING OF POLYMER BLENDS: POLYSTYRENE–POLY(METHYL METHACRYLATE)–POLY(STYRENE-*block*-METHYL METHACRYLATE) SYSTEM

Jaroslav HOLOUBEK

Institute of Macromolecular Chemistry, Academy of Sciences of the Czech Republic, 162 06 Prague 6, Czech Republic; e-mail: holoubek@imc.cas.cz

Received November 13, 2003
Accepted February 27, 2004

The time-resolved light scattering experiments have been conducted to investigate the kinetics of coarsening of phase-separated immiscible polymer blends with or without added block copolymer. The blends studied were polystyrene–poly(methyl methacrylate) mixtures with a diblock copolymer composed of the corresponding homopolymer blocks. The time evolution of the peak position $q_m(t,T)$ and the scattered intensity maximum $I_m(t,T)$ at q_m have been compared with the theoretically predicted values of exponents for various time scales of phase separation at various annealing temperatures.

Keywords: Diblock copolymers; Coarsening; Phase separation; Polystyrenes; Polyacrylates; Time-resolved light scattering.

For designing of new polymer materials by blending, basic understanding of the phase behaviour is necessary, involving phase equilibrium, kinetics of phase separation and kinetics of phase dissolution in polymer blends[1]. It is generally accepted that there are two mechanisms of phase separation, depending on where in the phase diagram the system is quenched, which can result in materials with quite different morphologies[2]. Quenches near the binodal, into the metastable region of the phase diagram result in the nucleation and growth (NG) mechanism, characterized by a more or less random array of droplets. Deeper quenches result in a mechanism known as spinodal decomposition (SD), which can possess a bicontinuous or a droplet morphology containing a characteristic length-scale[2]. Both mechanisms have been observed in a variety of binary and ternary polymer systems[3–15]. Coarsening of the structures formed by NG and SD can occur via interfacial and bulk diffusion of the components, droplet coalescence due to Brownian motion and, in some cases, surface-tension-driven hydrodynamic flow. Coarsening processes are inherently nonlinear, and analytical solutions of the governing equation are not yet known. The time depend-

ence of the scattering-intensity maximum (I_m) and wavevector maximum (q_m) at intermediate and late stages of the phase separation in a binary blend is often expressed as scaling laws[16,17]

$$q_m(t,T) \cong t^{-\alpha} \quad (1)$$

$$I_m(t,T) \cong t^{\beta} . \quad (2)$$

The exponential values of Eqs (*1*) and (*2*) fulfil the relationship $\beta = 3\alpha$ as a result of dimensionality arguments. The exponent α has a typical value around 1/3 at the intermediate stage and unity at the late stage of phase separation[16–21].

When a peak was present in the scattering function, the time dependences of the peak height, $I_m(t)$, and peak position, $q_m(t)$, were analyzed. The peak position dependence was fitted with a function of the form of Eq. (*1*) to obtain the coarsening exponent, α, which was compared with theoretical values. Since it is predicted that the late stages of growth are characterized by self-similarity of the structure (dynamic scaling)[22,23], the scaled structure function was constructed from the measured scattering functions, which will be mentioned in the Theoretical Background part in more detail.

Smaller coarsening exponents, most commonly taking the value of 1/4, have been predicted in a pre-asymptotic regime[7,10–12,14] and in the case where the interfacial width is so large that the interface introduces an extra length-scale into the system[7,10,13–15]. When the droplet size is approximately equal to the droplet separation, a coarsening exponent of 1/3 is predicted for the droplet coalescence mechanism[24]. However, when the separation is larger than the droplet size, the exponent becomes lower because of the lower collision frequency[24–26]. An exponent of unity is predicted for the hydrodynamic coarsening mechanism[18] where convective flow is coupled with droplet motion to accelerate the rate of coarsening. The lowest values (≈1/10) in liquid systems, however, have been observed in NG systems where the droplets are widely spaced and collisions are rare[25]. These findings demonstrate the need for a detailed examination. The aim of the present work was to probe the coarsening mechanism and kinetics in a ternary polymer by time-resolved light scattering experiments, image analysis and SEM. The blends studied were polystyrene–poly(methyl methacrylate) (PS–PMMA) mixtures with admixed diblock copolymer composed of the corresponding homopolymer blocks.

THEORETICAL BACKGROUND

Scattering Function

The scattering functions for SD samples possessed the form predicted by Furukawa[22,23] for a droplet structure with a negligible interfacial width formed from an off-critical quench

$$I(q) \approx [1 + (\gamma/2)q^2]/[(\gamma/2) + q^\gamma] , \quad (3)$$

where $\gamma = d + 1$, d being the dimensionality of the system ($d = 3$ in the present case because the droplet size was much smaller than the sample dimensions). The occurrence of dynamic scaling of the scattering function at the final stage of coarsening in the SD samples agrees with numerical simulations of phase separation, which show dynamic scaling in the asymptotic coarsening regime in the systems that coarsen by the diffusive mechanism[10], where the structure evolution can be described by a simple scaling law $R(t) \approx t^\alpha$. The evidence that a gradual movement toward the equilibrium compositions occurred was provided by the tendency of the peak height (which is directly related to the composition difference between the phases for the SD samples) toward a constant value at the late stages of the current experiments. The scaled structure function of Furukawa[20] (Eq. (*3*)) has been introduced to explain the scattering profiles (dimensionality $d = 3$)

$$I(q)/I_m(q) \approx c_1(q/q_m)^2/[c_2 + (q/q_m)^4] , \quad (4)$$

where c_1 and c_2 are constants.

Similarly, the plot of

$$I(q)/I_m(q) \approx c_3(q/q_m)^2/[c_4 + (q/q_m)^6] \quad (5)$$

has been used to find the best fit, where c_3 and c_4 are again constants. The asymptotic exponent –4 is characteristic of sharp domain/matrix interfaces at high scattering vectors $q >> q_m$ (the Porod law[2]).

Coarsening Mechanism: Structural Aspects of Power-Law Dependence

The influence of the system character on the coarsening behaviour of dispersed particles is discussed[27] for a polydispersed system with a Debye–Bueche type of the angular dependence of the scattering intensity (I_m occurring at $q = 0$). The coarsening probability p is a complex function of Φ,

η_m and R, where Φ is the volume fraction of the minor component, η_m is the viscosity of the matrix phase and R is mean particle radius. The proportionality constant k in the relation $R = kt^{\alpha}$ is related to the characteristic constants Φ, η and Γ (Γ is the interfacial tension) and does not change with time. An increased volume fraction, interfacial tension, or decreased viscosity of either phase increase the proportionality constant, which causes the dispersed particles to grow fast. The growth exponent α is related to the probability of coarsening p, i.e., $\int p\,dt \approx t^{\alpha}$. During an increase in particle radius R with time t, the probability p decreases, which results in the decrease in the growth exponent α. It is easy to understand that the Brownian motion reduces the increasing particles radius. Meanwhile, the distance between two neighboring particles increases with R, which implies decreasing p. However, the resulting effect strongly depends on the speed of changes of R. The faster is the R increase, the slower is the increase of the integral $\int p\,dt$ (i.e., the smaller is the exponent α). There is a gradual change in the shape of the $R = kt^{\alpha}$ curves because of different volume fractions. The time dependence of the mean particle radius is almost linear for small volume fractions. For large volume fractions, the exponent α is less than 1, ca. 0.8 for $\Phi = 0.4$. It is necessary to point out that this theoretical model is derived from immiscible polymer blends with dispersed particle structures in the matrix (sea-island structure). Thus the classic 1/3 growth law does not hold for this system[28,29]. A large interfacial tension accelerates the draining and merging stages, thus making the particles grow faster.

EXPERIMENTAL AND MATERIALS

PS (M_w 9.0 × 10^4 g/mol, Polyscience), polydispersity index (PI) = M_w/M_n = 1.06 , PMMA (M_w 7.5 × 10^4 g/mol, Pressure Chem.), PI = 1.04 and PS-*b*-PMMA copolymer (M_w 8.0 × 10^4 g/mol), PI = 1.06 were used. The glass temperatures are: T_g (PS) = 99 °C, T_g (PMMA) = 105 °C. Time-resolved light scattering (which probes the q range from 0.2 to 30 μm^{-1}, where q is the wavenumber of fluctuations) has been widely used to examine the phase separation kinetics in polymer blends and solutions[1,30]. Details of the instrument are described elsewhere[30]. First, PMMA and PS polymers were dissolved in benzene in the 30/70 weight ratio (PS–PMMA). The solution was filtered with a 1 μm Teflon filter. The films were prepared by casting from 7% benzene solution on Petri dishes 2 cm in diameter. The films were dried at 90 °C in vacuum for 1 day. The sample holder consisted of two electrically heated quartz plates with a copper shell insert defining the sample thickness (ca. 50 μm). The holder temperature was controlled to within ±0.1 °C. The scattered intensity was detected with a CCD camera. The time regimes were selected from a time table in dependence on the temperature changes from the starting to final temperatures. The highest frame speed was ca. two frames per second. The scattering angles, θ, which are accessible in this experiment are 0.5–42°, and the corresponding wavevectors ($q = (4\pi R/\lambda)\sin(\theta/2)$) are 0.0002–0.012 nm^{-1}. This corresponds in the real space to the domains of size $L = 2\pi/q$, i.e. between 0.5 and 30 μm. We

used a standard laser (He-Ne, 15 mW) of λ = 632.8 nm. We smoothed the noisy data by averaging them over circular shells of various thickness; i.e., each point shown in the plot of $I(q,t)$ vs q has been integrated over the q range (with angular resolution ca. 0.1°) and over the azimuthal angles 0–2π. The range of q integration could be varied or even overlapped for individual points.

RESULTS AND DISCUSSION

We present here the results for two systems: (*1*) PS–PMMA blend (30/70) and 4% of diblock copolymer PS-*b*-PMMA and (*2*) PS–PMMA (30/70) blend. It has been shown[31,32] that a blend of two immiscible polymers obtained by casting from a non-selective solvent displays a relatively "fine" systems of domains with typical dimensions in the range of several microns. The SEM micrographs of the PS–PMMA blend with 4% of block copolymer PS-*b*-PMMA are given in Fig. 1. The left part shows the free film surface with PS domains in the PMMA matrix. In the right part is the sub-surface morphology with the PMMA matrix eliminated by acetic acid etching[33].

The presence of a peak in NG colloidal and polymer systems above a certain droplet volume fraction has been explained by the presence of a depletion layer around the droplets that causes further nucleation to occur in preferred regions[25,34–41]. When the droplet volume fraction is high enough, this effect leads to a correlated morphology[25,34–38] (cf. Fig. 1). In the light scattering experiment, one thus observes a peak of intensity at a nonzero scattering vector.

The three main ways how the NG peak can be distinguished from the SD peak are a different profile of the peak height evolution with time, initial movement of the NG peak to higher scattering vectors, and lower coarsening exponents from the NG peak[34–40].

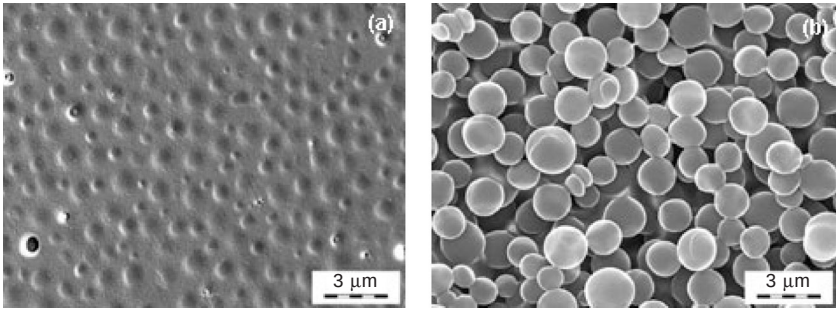

FIG. 1
Scanning electron micrographs of PS–PMMA (30/70), 4% of copolymer: a surface of the film, b subsurface area with PMMA removed with acetic acid

The size scale of the morphology observed by comparing the corresponding q_m for samples with and without the copolymer (cf. Fig. 2) was found to decrease with added diblock copolymer (cf. a larger q_m value for a sample with copolymer) and corresponds very well with the sizes from SEM micrographs (cf. Fig. 1).

The coarsening kinetics was monitored by plotting the time dependence of the peak position in scattering function (q_m). Power-law coarsening kinetics were observed in all samples, although the exponents of the power law observed over the time range studied varied systematically with annealing temperature. The variation of q_m with time in semilogarithmic plot is shown in Fig. 2. The various coarsening exponents measured in various regimes are shown in Fig. 3.

When the matrix viscosity increases, both the draining rate and merging rate decrease, which slows down the particle growth. The predictions and experimental data also show the effect of temperature on coarsening. Raising the temperature can not only decrease the viscosity of both phases but also enhance the Brownian motion. The exponent α becomes smaller when the interfacial tension increases[42]. Therefore the change in interfacial tension with temperature will affect coarsening, but the influence is negligible compared to other effects.

The block copolymer probably tends to slow down the transport of homopolymers across the interfaces because of accumulation of the copolymer at the interface. The formation of an interfacial layer could induce a

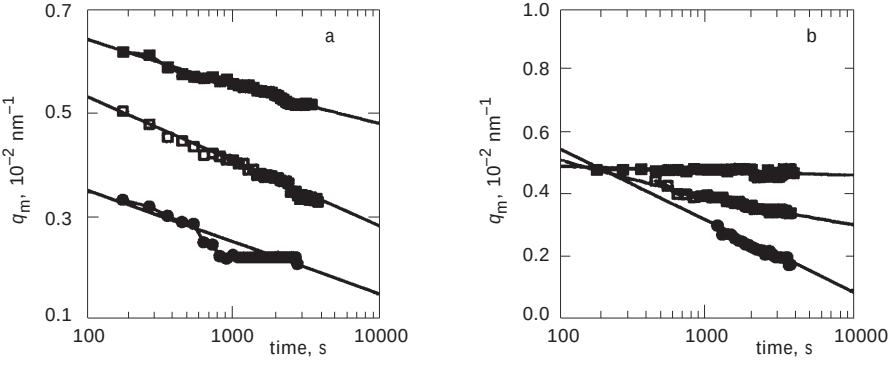

FIG. 2
Evolution of the peak position q_m with time for samples PS–PMMA (30/70) at various annealing temperatures (in °C): 130 (■), 160 (□), 180 (●); a with 4% of block copolymer, b without addition of block copolymer

strong inhibition mechanism of droplet coalescence similar to that in thin film[43,44]. Therefore, the dimensional growth is retarded.

Intensity plots with values $I(q_m)$ for samples with and without the copolymer are given in Fig. 4 for annealing temperatures T = 130, 160 and 180 °C. The power law exponents obtained from the fit in Fig. 4 are significantly lower than the theoretically predicted values. This might be influenced by the proximity of the T_g temperatures of both homopolymers, but further tests of this hypothesis are necessary. Experimental results for blends without the copolymer are presented in Figs 4b, 4d, 4f. They show larger starting I_m values in comparison with the blends with the copolymer (cf. Figs 4b, 4d, 4f). The scattered intensity is proportional to the size and number of scattering objects and the density difference between them and the surrounding medium. This agrees well with the expected "homogenization" effect of the copolymer.

The power-law dependence of $I(q_m)$ on time is fulfilled only for samples with the copolymer (Eq. (*2*)). The predicted power growth law is indicated in Fig. 4 by solid curves. For higher annealing temperatures, T = 160 and 180 °C, the shape of the I_m vs time curves corresponds to the power-law type, but the exponents of the power law (ca. 0.15) are much lower than the predicted value β = 0.75–1. For the lowest annealing temperature T = 130 °C, the power law dependence of growing I_m on time is evidently not fulfilled.

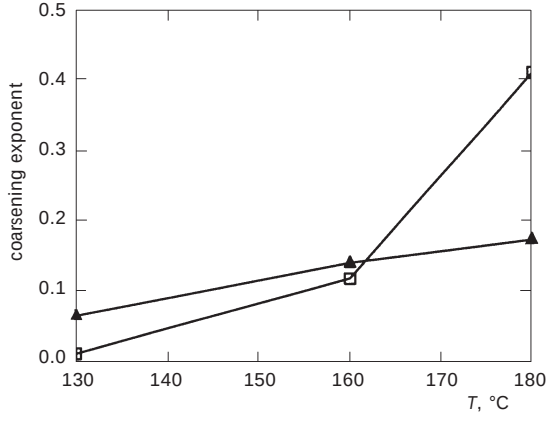

FIG. 3
Comparison of coarsening exponents measured for samples PS–PMMA (30/70) with 4% of block copolymer (▲) and without block copolymer (□)

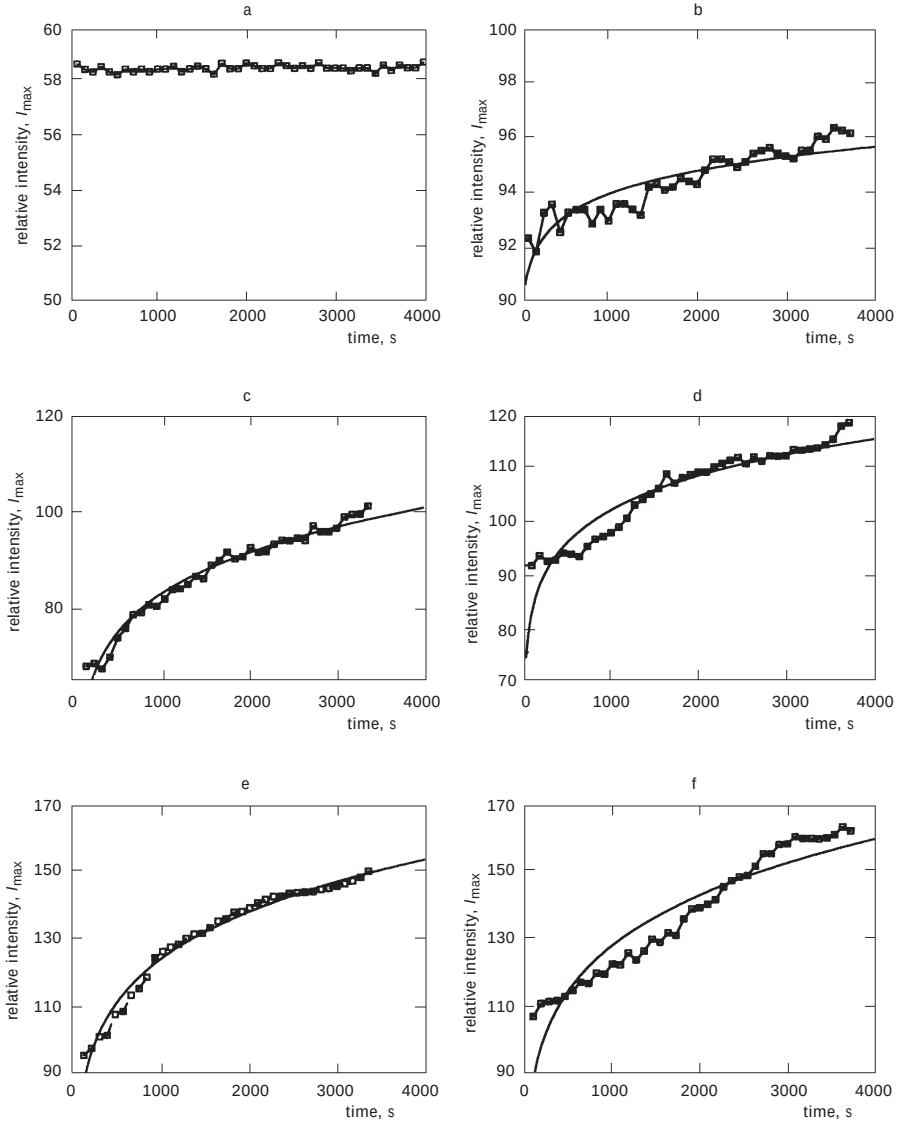

FIG. 4

The time dependence of I_m for the PS–PMMA (30/70) blends at temperatures (in °C): 130 (a, b), 160 (c, d) and 180 (e, f). Samples with 4% of block copolymer are in the left column (a, c, e).

Figures 4b, 4d, 4f illustrate almost linear dependence of growing I_m on time. It is evident that addition of the block copolymer suppresses the scattering intensity, but the scattering maximum data are not consistent with $\beta = 1$ at the intermediate and late stages of phase separation. This discrepancy indicates that the time dependence of the scattering maximum does not seem to follow the theoretical scaling predictions. For a clear comparison, the normalized scattering intensities, I/I_m vs q/q_m , for both the blends are plotted in Fig. 5.

For all studied blends, the normalized scattering profiles at the intermediate stage are to a certain extent self-similar and collapsing into a single master curve as a function of time, as shown in Fig. 5. The scattering intensity profiles show a slope of –4 for $q/q_m > 1$ at lower annealing temperatures, 140 and 160 °C. On the other hand, at the highest temperature, 180 °C, the slope is less steep than the slopes of the two previous cases. This can be interpreted as an indication of the formation of fuzzy boundaries caused by accumulation of diblock copolymers at the interfaces of the phase-separated domains or by growth of small new domains formed in the original domains as well as in the original matrix.

The absence of dynamic scaling at the early stages can be explained by the finite time required by the phases to reach their equilibrium compositions, which is expected to prevent scaling even when the interfaces are sharp[24]. The reason for the absence of complete dynamic scaling in the final coarsening regime is uncertain. Convective effects lead to departures from scaling[45,46]. Although convection did not significantly affect the coarsening kinetics over the time period studied, a small amount possibly occurred, which was sufficient to prevent the structure from evolving in a self-similar manner. Another possibility would be that the sample was simply left for an insufficient time to reach the asymptotic scaling regime[47]. Scaling of the scattering function in the NG samples did not occur completely because nucleation of new droplets caused continuous changes in the length-scale of the morphology, and the system did not obey the $R(t) \approx t^{\alpha}$ scaling relationship.

A broadening of the normalized light scattering profiles at $T = 180$ °C for both the blends was observed (cf. Figs 5e, 5f). This implies that the distribution of the domain size gradually broadened with time.

CONCLUSIONS

The coarsening process was studied by systematically annealing two blend systems, at a fixed composition, at different temperatures. Nucleation and

growth of particulate systems was characterized by time evolution of $I_m(q,t)$ and $q_m(t)$ at various temperatures. A self-similarity of structures was observed at the late stages of coarsening. Dynamic scaling did not occur at the early stages of coarsening because the phases had not attained their equilib-

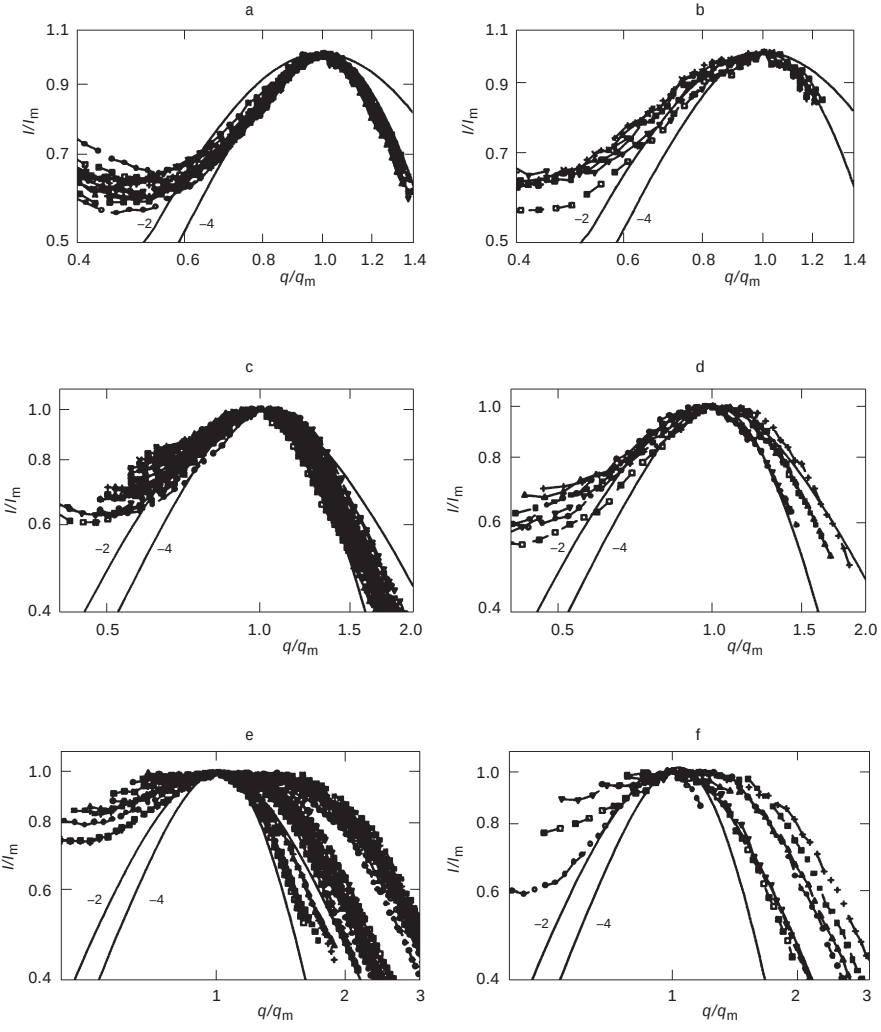

FIG. 5

The time dependence of normalized scattering intensity I/I_m for PS–PMMA (30/70) blends at temperatures (in °C): 130 (a, b), 160 (c, d) and 180 (e, f). Samples with 4% of block copolymer are in the left column (a, c, e)

rium compositions, shown by a gradual change in the peak height toward an asymptotic limit. At the early stages of coarsening of the samples, the interface was sufficiently diffuse to cause deviations from Porod's law. Coarsening laws of the form $R(t) \approx t^{\alpha}$ were obeyed by the samples. Coarsening exponents with values between 1/10 and 1/3, including in some cases a transition to a temporary faster coarsening regime, were measured in the samples. The low coarsening exponents were a consequence of the loss of mobility of the components caused by the proximity of the glass transition temperature of both components. At all times of nucleation and growth of samples, the coarsening exponent was lower than 1/3 because coarsening occurred via droplet coalescence and the droplet size was significantly smaller than the droplet separation. A coarsening exponent of 1/3 was measured at the final stage of coarsening once the droplet size was in the range of the droplet separation. Systems containing block copolymers were shown to ripen with a power law exponent less than 1/3, indicating stabilization of the system[48].

The model predictions[27] agree well with our experiments and are consistent with other published experimental data within a tolerable error limit. The increasing rate of particle radius with time depends on the system parameters. In general, a low volume fraction, low interfacial tension, and high matrix viscosity result in a nearly linear relation of the dispersed particle radius and the annealing time ($R \approx t$). Otherwise, the relation deviates from linearity, with the exponent α of $R = kt^{\alpha}$ less than 1.

The author gratefully acknowledges the support of the Grant Agency of the Czech Republic (grant No. 203/02/1262) and of the Grant Agency of the Academy of Sciences of the Czech Republic (grants No. A4050305 and No. A1050201). The author is grateful to Ms J. Hromádková for her skilful help with SEM images.

REFERENCES

1. Gunton J. D., Migaud M. S., Sahni P. S. in: *Phase Transition and Critical Phenomena* (C. Domb and J. L. Lebowitz, Eds). Academic Press, New York 1983.
2. Strobl G.: *The Physics of Polymers*. Springer, Berlin 1996.
3. Lifshitz I. M., Slyozov V. V.: *J. Phys. Chem. Solids* **1961**, *19*, 35.
4. Tokuyama M., Kawasaki K.: *Physica A (Amsterodam)* **1984**, *123(2-3)*, 386.
5. Huse D. A.: *Phys. Rev. B: Condens. Matter* **1986**, *34*, 7845.
6. Mazenko G. F.: *Phys. Rev. B: Condens. Matter* **1991**, *43*, 8204.
7. Mazenko G. F.: *Phys. Rev. Lett.* **1989**, *63*, 605.
8. Toral R., Chakrabarti A., Gunton J. D.: *Phys. Rev. Lett.* **1988**, *60*, 2311.
9. Chakrabarti A., Toral R., Gunton J. D., Muthukumar M.: *Phys. Rev. Lett.* **1989**, *63*, 2072.
10. Rogers T. M., Elder K. R., Desai R. C.: *Phys. Rev. B: Condens. Matter* **1988**, *37*, 9638.

11. Chakrabarti A., Toral R., Gunton J. D.: *Phys. Rev. B: Condens. Matter* **1989**, *39*, 4386.
12. Rogers T. M., Desai R. C.: *Phys. Rev. B: Condens. Matter* **1989**, *39*, 11956.
13. Bray A. J.: *Phys. Rev. Lett.* **1989**, *62*, 2841.
14. Mouritsen O. G.: *Phys. Rev. B: Condens. Matter* **1985**, *31*, 2613.
15. Mazenko G. F., Valls O. T., Zannetti M.: *Phys. Rev. B: Condens. Matter* **1988**, *38*, 520.
16. Akcasu A. Z., Klein R., Hammouda B.: *Macromolecules* **1993**, *26*, 4136.
17. Langer J. S., Baron M., Miller H. D.: *Phys. Rev. A* **1975**, *11*, 1417.
18. Siggia E. D.: *Phys. Rev. A: At., Mol., Opt. Phys.* **1979**, *20*, 595.
19. Rao M., Kalos M. H., Lebowitz J. L., Marro J.: *Phys. Rev. B: Solid State* **1976**, *13*, 328.
20. Furukawa H.: *Physica A (Amsterdam)* **1984**, *123*, 497.
21. Binder K., Stauffer D.: *Phys. Rev. Lett.* **1974**, *33*, 1006.
22. Furukawa H.: *Adv. Phys.* **1985**, *34*, 703.
23. Furukawa H.: *J. Appl. Crystallogr.* **1988**, *21*, 805.
24. Tanaka H.: *J. Phys.: Condens. Matter* **2000**, *12*, 207.
25. Tanaka H., Yokokawa T., Abe H., Hayashi T., Nishi T.: *Phys. Rev. Lett.* **1990**, *65*, 3136.
26. Furukawa H.: *Phys. Rev. A: At., Mol., Opt. Phys.* **1981**, *23*, 1535.
27. Yu W., Zhou C., Inoue T.: *J. Polym. Sci., Part B: Polym. Phys.* **2000**, *38*, 2378.
28. Mirabella F. M.: *J. Polym. Sci., Part B: Polym. Phys.* **1994**, *32*, 1205.
29. Mirabella F. M., Barley J. S.: *J. Polym. Sci., Part B: Polym. Phys.* **1994**, *32*, 2187.
30. Holoubek J., Koňák Č., Štěpánek P.: *Part. Part. Syst. Charact.* **1999**, *16*, 102.
31. Christopoulou V., Papanagopoulos D., Dondos A.: *J. Polym. Sci., Part B: Polym. Phys.* **1998**, *36*, 1051.
32. Lowenhaupt B., Hellmann G. P.: *Colloid Polym. Sci.* **1994**, *272(2)*, 121.
33. Walheim S., Bötau M., Mlynek J., Krausch G., Steiner U.: *Macromolecules* **1997**, *30*, 4995.
34. Eliçabe G. E., Larrondo H. A., Williams R. J. J.: *Macromolecules* **1998**, *31*, 8173.
35. Eliçabe G. E.: *Macromol. Theory Simul.* **1999**, *8*, 375.
36. Banfi G., Degiorgio V., Rennie A. R., Barker G.: *Phys. Rev. Lett.* **1992**, *69*, 3401.
37. Maugey J., Van Nuland T., Navard P.: *Polymer* **2001**, *42*, 4353.
38. Eliçabe G. E., Larrondo H. A., Williams R. J. J.: *Macromolecules* **1997**, *30*, 6550.
39. Rikvold P. A., Gunton J. D.: *Phys. Rev. Lett.* **1982**, *49*, 286.
40. Carpineti M., Giglio M., Degiorgio V.: *Phys. Rev. E: Stat. Phys., Plasmas, Fluids, Relat. Interdiscip. Top.* **1995**, *51*, 590.
41. Tromp R. H., Jones R. A. L.: *Macromolecules* **1996**, *29*, 8109.
42. Fortelný I., Živný A., Jůza J.: *J. Polym. Sci., Part B: Polym. Phys.* **1999**, *37*, 181.
43. Nakatani A. I., Sung L., Hobbie E. K., Han C. C.: *Phys. Rev. Lett.* **1997**, *79*, 4693.
44. Karim A., Douglas J. F., Satija S. K., Han C. C., Goyette R. J.: *Macromolecules* **1999**, *32*, 1119.
45. Tromp R. H., Rennie A. R., Jones R. A. L.: *Macromolecules* **1995**, *8*, 4129.
46. Butler M. F., Heppenstall-Butler M.: *Biomacromolecules* **2001**, *2*, 812.
47. Fialkowski M., Holyst M.: *J. Chem. Phys.* **2002**, *117*, 1886.
48. Russo A. P., Nauman E. B.: *J. Polym. Sci., Part B: Polym. Phys.* **2000**, *38*, 1301.